Synthesis and characterization of alginate-polyacrylic acid/multiwalled carbon nanotubes composite with efficient removal for nigrosine dye

Mohamed I. A. Ibrahim[a,b*], Islam M. Abdelmonem[c], Laila A. Mohamed[a], Mohamed A. Gizawy[d], E. Metwally[c]

[a]*National Institute of Oceanography and Fisheries, NIOF, Egypt.*

[b]*Hiroshima Synchrotron Radiation Center, Hiroshima University, Kagamiyama, Higashi-Hiroshima, Hiroshima 739-0046, Japan*

[c]*Nuclear Chemistry Department, Hot Labs Center, Egyptian Atomic Energy Authority, P.O. Box 13759, Cairo, Egypt.*

[d]*Labeled Compounds Department, Hot Labs Center, Egyptian Atomic Energy Authority, P.O. Box 13759, Cairo, Egypt.*

*Corresponding Author
Mohamed I. A. Ibrahim
Assistant professor of Marine Chemistry,
Laboratory of Marine Chemistry, National Institute of Oceanography and Fisheries, NIOF, Egypt.
Hiroshima Synchrotron Radiation Center, HiSOR, Hiroshima University, Japan.
Tel: +2-03-480-1553 / +81-82-424-6293
Fax: +2-03-480-1449 / +81-82-424-6294
ORCID: 0000-0001-6190-5899
Scopus Author ID: 57195522700
E. mail: ibrahimmohamed2030@gmail.com
m.ibrahim@niof.sci.eg
ibra2020@hiroshima-u.ac.jp

Synthesis and characterization of alginate-polyacrylic acid/multiwalled carbon nanotubes composite with efficient removal for nigrosine dye

Abstrat: The current study detailed the efficacy of a simply prepared alginate-polyacrylic acid/functionalized multiwalled carbon nanotubes (Alg-PAA/f-MWCNTs) composite for adsorption of nigrosine dye (acid black II) from aqueous environments. Firstly, preparation of the Alg-PAA/f-MWCNTs composite was achieved *via* gamma radiation-induced template polymerization of AA onto the Alg/f-MWCNTs surface. The maximum grafting efficiency (GE%) of AA onto the surface of Alg/f-MWCNTs was ~ 82% under the optimized conditions: (2.5 wt% Alg, 30 wt% AA, 0.5 wt% f-MWCNTs, 0.6 wt% *N*,*N'*-methylenebisacrylamide (NMBA), and irradiation dose ~ 20 kGy). The structural characteristics, thermal features as well as the morphological appearance of the Alg-PAA/f-MWCNTs composite were validated using different analyses including FTIR, TGA, DTA, XRD and SEM. Additionally, the composite exhibited uniform particle size distribution (~ 150.7 nm), point of zero charge at pH = 6.28, and negative Zeta potentials of a minimum at pH = 2. The adsorption batch experiments showed good adsorption capacity for the nigrosine dye from their aqueous media with adsorption efficiency up to 83% using the batch technique at pH = 2.0 for 420 min. The adsorption of nigrosine dye onto Alg-PAA/f-MWCNTs is favourable thermodynamically, obeying the Freundlich isotherm model and controlled by a chemisorption mechanism. Additionally, the composite showed a good regeneration ability up to five times with almost the same removal % (~ 80%). The results demonstrated that the Alg-PAA/f-MWCNTs composite could be a promising candidate for the removal of nigrosine dye from industrial aqueous environments.

Keywords: biosorption; nigrosine; alginate-polyacrylic acid/multiwalled carbon nanotubes; kinetics; thermodynamics

Introduction

Recently, synthetic dyes have been widely utilized in many processing industries (e.g., inks, textiles, cosmotics, rubbers, plastics, leather, papers, food, etc.).[1, 2] Dyes are classified into anionic dyes, cationic dyes, and non-ionic ones of dispersed behaviours.[3] The majority of the dyes are of synthetic origin, possessing complex structures, which make them more stable and less biodegradable. Because of their high solubility and toxicity, dyes are an influential source of water pollutants even at low concentrations (< 1.0 ppm),[4] which adversely affect the aquatic life and food web. Several studies have offered the removal of dyes from wastewaters. Numerous physical methods have been reported to reduce the hazard effects of the dye effluents such as reverse osmosis, ultra-filtration, ion exchange, coagulation and flocculation, photo-degradation, and adsorption.[5-7] Furthermore, several chemical processes such as photosensitized oxidation, adsorption, and photofenton's reactions have also been applied for removing dyes.[8-11] However the aforementioned methods are fairly effective in pollutants' removal, most of them suffer from transforming the dyes solution into solid forms which need further treatment. Among all methods, adsorption is considered as one of the promising and effective ways for removing dyes from polluted waters, producing waters of high quality. Adsorption principle has been successfully applied for the removal of several dyes including methylene blue (MB), rhodamine B, methyl orange, congo red, acid black II, disperse violet 26, methyl red, and crystal violet (CV), from wastewaters originating particularly from textile, cosmetic, leather, food, pharmaceutical, paint and varnish, pulp, and paper industries.[12-16]

Many studies highlighted the use of bio-sorbents (e.g., starch, alginate, chitin, chitosan, etc.) for removing dyes from wastewaters as eco-friendly, cost-effective, and commercially available adsorbents. Biopolymers are distinguished of being naturally

abundant, biodegradable, biocompatible, and exhibiting versatile chemical structures associated with the presence of various active functional groups, which contribute effectively towards the removal of dyes.[17] Unfortunately, biopolymers have been limited in various applications due to their weak mechanical properties, or gel formation. Additionally, natural polymers are not sufficient to remove the dyes from highly complex dye-containing wastewaters contaminated with different types of pollutants. To overcome limitations, the biopolymers should be subjected to a modification process, involving chemical or physical strategy, to increase their efficiency in removing dyes from complex wastewaters.[18] Radiation-induced graft polymerization offers a convenient method for modifying polymers, introducing new characteristics while preserving the original ones. Various radiation sources, such as electron beams, UV, and γ-radiation, can be employed for this process.[19] When ionizing radiation interacts with matter, particularly through the atomic shell's electrons, it generates reactive species, predominantly free radicals, leading to ionization or excitation.[20] The advantages of radiation-induced graft polymerization include its simplicity, the ability to control graft content and reaction parameters, and compatibility with commercially available polymer substrates. Additionally, this method avoids the use of potentially hazardous materials such as catalysts, additives, initiators, or organic solvents.[21, 22] Poly(ethersulfone) membranes underwent surface modification through a straightforward one-step process. The membranes were immersed in aqueous solutions containing diverse low-molecular-weight molecules with varied hydrophilic functionalities, followed by electron beam treatment.[23] Gamma irradiation crosslinking was also applied to prepare polyacrylic acid-polyvinyl alcohol-polyethylene oxide [p(AAc/PVA/PEO)] hydrogel membranes. This process creates a three-dimensional network structure, or hydrogel, by creating chemical links between polymer chains.[24]

Alginate, a naturally occurring anionic polymer, has been extensively researched and applied in various biomedical contexts due to its attributes of low toxicity, biocompatibility, and cost-effectiveness[25]. On the other hand, multi-walled carbon nanotubes (MWCNTs) have garnered a significant attention as additives, given their unique capabilities in adsorption, catalysis, thermal conductivity, mechanical strength, and electrical conductivity.[26] The process of functionalizing MWCNTs enhances their reactivity, solubility, and opens new avenues for chemical modification. Moreover, the introduced functional groups serve as anchor points, facilitating the bonding of two entities and enabling further derivatization through chemical interactions with additional functional groups.[27] Thus, alginate-based composites have been extensively researched for the removal of synthetic dyes from aqueous solution. Benhouria et al. (2015) developed bentonite-alginate beads to eliminate methylene blue, achieving a maximum monolayer adsorption capacity of 756.97 mg/g at 30°C after six regeneration cycles.[28] Fan et al. (2013) synthesized graphene oxide/sodium alginate/polyacrylamide (GO/SA/PAM) composite hydrogels, which effectively adsorb cationic and anionic dyes from wastewater.[29] Sui et al. (2012) studied ionic dye adsorption on calcium alginate and multi-walled carbon nanotube (CA/MWCNT) composite fibers, finding MWCNTs increased the adsorption capacity and improved the removal rate.[30] Wang, Wang, and Wang (2013) developed NaAlg-g-p(AA-co-St)/organo-I/S nanocomposite absorbents to eliminate MB, achieving a fast adsorption capacity of 1843.46 mg/g.[31]

Nigrosine dye (acid black II) is an anionic azo dye, a mixture of black dyes (i.e., CI 50415, and solvent black 5), synthesized by heating a mixture of aniline, nitrobenzene, and aniline hydrochloride in presence of copper or iron as a catalyst. The sulfonated form of nigrosine dye is more soluble in water and often used for dying textiles, leather, and as marker-pen inks as well as in the biology field for negative staining bacteria.[10, 32] The

choice of nigrosine acid black II as the model dye is related that it is a traditional water-soluble dye, in addition to being used as a common analytical reagent. Consequently, a significant amount of nigrosine dye as wastewater is discharged into aquatic environments from laboratories, factories, etc. The current study is one of rare work that focused on the removal of a traditional nigrosine dye from an aqueous solution using a simply designed Alg-PAA/f-MWCNTs composite. Firstly, the composite was prepared through the gamma radiation-induced polymerization of AA onto the Alg/f-MWCNT surface, followed by the structural validation of the composite using FTIR, SEM, TGA, XRD and DTA. Then, the factors affecting the nigrosine removal *via* the adsorption process (e.g., pH, time, nigrosine concentration, and temperature) were examined using batch methods. Modelling of the kinetics, equilibrium isotherms, thermodynamics, and regeneration of the prepared composite were also investigated.

Material and methods

General

All chemicals and solvents of highest purity grades were used in performing the synthesis and experimental part: sodium alginate (Alg; Sigma-Aldrich, Germany), acrylic acid monomer (AA; Merck-Schuchardt, Germany), multi-walled carbon nanotube (MWCNTs; EMFUTUR, Spain), and *N*,*N*′-methylenebisacrylamide (NMBA; Merck, Germany).

Synthesis of the Alg-PAA/f-MWCNTs composite

The Alg-PAA/f-MWCNTs composite was synthesized through multiple consecutive steps in a good overall yield as illustrated in **Figure 1**. Firstly, chemical oxidation of the MWCNTs was carried out using a strategy described elsewhere.[26, 33] The yielded f-MWCNTs were ultrasonicated in distilled water for 0.5 h before the addition of sodium alginate, and the suspension was heated at 50°C until a homogeneous solution was

158 obtained. Afterward, AA then NMBA (crosslinker) were added to the solution under
159 agitation at 50°C until homogeneity was observed.

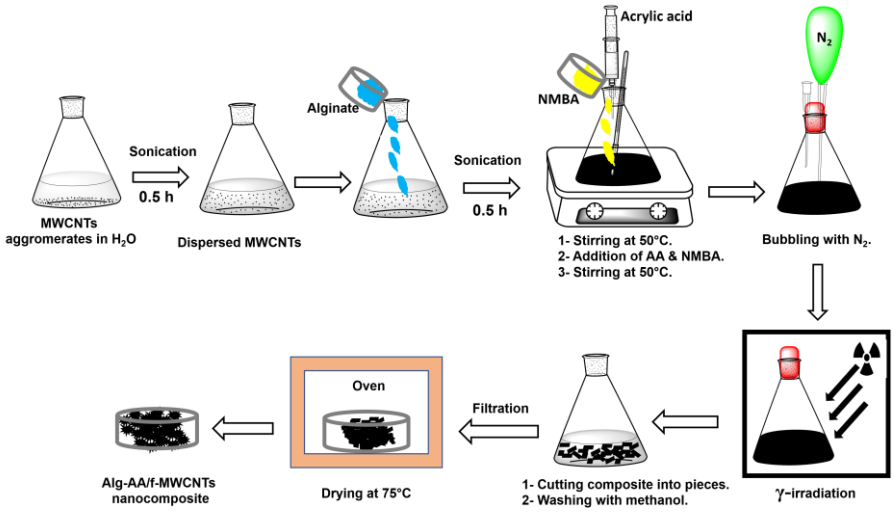

160

161 **Figure 1.** Schematic representation of a stepwise procedure for the synthesis of Alg-
162 PAA/f-MWCNTs.

163 The mixture was bubbled with nitrogen gas to discard the oxygen before subjection to
164 polymerization by γ-radiation. The polymerization was achieved at ambient temperature
165 using γ-radiation with an average dose rate of ~ 1.05 kGy/h using a ^{60}Co–γ-ray field to
166 reach the optimum radiation dose (Cobalt-60 gamma cell MC-20, Cyclotron Project,
167 Inshas, Egypt). Finally, the obtained nanocomposites were divided into tiny pieces then
168 washed with methanol, and the resultant grafted material (Alg-PAA/f-MWCNTs) was
169 filtered and dried at 75°C till a constant weight was obtained, then was stored for later
170 evaluations.[34]

171 The grafting percentage and grafting efficiency were computed using formulas (1) and
172 (2), respectively.[35]

173 $$\text{Grafting percentage (G\%)} = \frac{(W_g - W_o)}{W_o} \times 100 \qquad \text{Eq. (1)}$$

174 $$\text{Grafting efficiency (GE\%)} = \frac{(W_g - W_o)}{W_m} \times 100 \qquad \text{Eq. (2)}$$

175 Where W_o, W_g, and W_m are the weights of polymer backbone (Alg/f-MWCNTs), graft
176 polymer (Alg-PAA/f-MWCNTs), and monomer (AA), respectively.

Characterization of the Alg-PAA/f-MWCNTs composite

The structural features of the synthesized Alg-PAA/f-MWCNTs composite were emphasized by Fourier transform infrared (FTIR), thermogravimetric (TGA) and differential thermal analyses (DTA), X-ray diffraction (XRD) analysis (D_2 Phaser-Bruker, Germany), as well as scanning electron microscope (SEM). The chemical functionality of the nanocomposite was identified using FTIR in the range (4000 – 400 cm^{-1}) with 4 cm^{-1} resolution by KBr disc method using a Shimadzu infrared spectrometer (BOMEM, FTIR, Japan). The thermal analyses of the composite using the TGA and DTA involved heating the composite at a rate of 20°C/min (Shimadzu DTG-60 thermal analyzer, Japan). The microstructure morphology of the composite surface was investigated using a scanning electron microscope (JEOL-JSM 6510 LA, Japan). Additionally, the Zeta potential analysis and particle size distribution of composite were determined (Malvern Zeta nano-sizer ZSP ZEN 5600).

Adsorption studies

Preparation of acid black II dye solution

A stock of acid black II dye solution (1000 mg/L) was prepared by dissolving 1.0 g of dye in 1.0 L deionized water. Standard solutions of acid black II dye (5.0,10.0,15.0, and 20.0 mg/L) were prepared by diluting (0.25, 0.5, 0.75, and 1.0 mL) of acid black II stock solution into a 50 mL measuring flask and completed to mark with deionized water.

Batch adsorption experiments

The reaction mixture was prepared by adding exact weights of the adsorbent into 50 mL glass bottles containing 25 mL of the prepared solution. All experiments were carried out using a digital laboratory orbital shaker machine to get the optimum conditions (pH, contact time, dye concentration, and temperature). The samples were filtered for separation of adsorbent. The residual concentrations of dye were measured by a UV-

Visible spectrophotometer at a wavelength of 573 nm. The removal percentage of acid black II dye was calculated using equation (3),[36]

$$\% \text{ Removal } = \frac{(C_o - C_e)}{C_o} \times 100 \qquad \text{Eq. (3)}$$

While (C_o) and (C_e) are the concentrations (mg/L) of the dye at zero time (t = 0) and equilibration time (t), respectively. The adsorption capacity of (Alg-PAA/f-MWCNTs) composite at equilibrium Q_e (mg/g) was calculated from equation (4),[37]

$$Q_e = \frac{(C_o - C_e)\ V}{m} \qquad \text{Eq. (4)}$$

Where C_e is the equilibrium concentrations of dye (mg/L), V is the volume of the solution (L) and m is the mass of adsorbent (g).

Effect of the adsorption parameters on the removal of dyes

pH of solution

The effect of pH on Alg-PAA/f-MWCNTs composite was studied by adjusting the acid black II solutions at different values (pH = 2.0 to 12.0), using 0.05 g as adsorbent dose. The experiment was performed at an agitation rate of 200 rpm for 420 min at room temperature, and an initial dye concentration of 10 mg/L, to obtain the pH value of the highest efficient capacity. The initial pH values of aqueous solutions were adjusted by using HCl (0.1 M) or NaOH (0.1 M) solutions, and fresh solutions were prepared for each experiment.

The point of zero charge of the prepared composite was also determined. In brief, about 0.05 g of the composite was added to an array of 125 stoppered bottles. A 50 mL of different pH buffer solutions (pH = 1.0 – 12.0) were poured into the stoppered bottles under shaking at 200 rpm at room temperature. The pH of the solutions was controlled using 1.0 N HCl, 1.0 N NaOH and acetate buffer. Then, the pH of each bottle was measured using pH meter after 24 hrs. The pH difference ($\Delta\, pH$) between the initial and

final values were calculated using the equation: $\Delta\, pH = pH_{Initial} - pH_{Final}$ which then plotted against the $pH_{Initial}$. The point of zero charge (pH_{pzc}) of the composite is the pH corresponds to $\Delta\, pH$ = zero.[38]

Contact time

For determination of the optimum contact time, the adsorption capacities of the Alg-PAA/f-MWCNTs composite for acid black II dye was tested at time intervals (30, 60, 90, 120, 180, 360, 420, 960, and 1440 min), agitation speed (200 rpm), pH 2.0, adsorbent dose (0.05 g), and initial dye concentration 10.0 mg/L at room temperature.

Initial dye concentration

The optimum initial dye concentration was determined by evaluating the adsorption capacities of the composite towards the dye at various concentrations (0.5,1.0, 2.0, 5.0, 10, 15, 20, 50, and 100 mg/L) at constant agitation speed (200 rpm), pH 2.0, adsorbent dose (0.05 g), during agitation time of 420 min at room temperature.

Temperature

The experiments help to follow the adsorption extents of acid black II dye on the composite surfaces with temperature variations. The experiments were performed using an initial dye concentration of 10 mg/L at five different temperatures (30, 40, 50, and 60 °C), agitation speed (200 rpm), pH 2, and adsorbent dose (0.05 g) for 180 min.

Adsorption kinetics, isotherm, and thermodynamics

Adsorption kinetics were modeled and compared using pseudo-first-order (PFO), pseudo-second-order (PSO), and the intraparticle diffusion model (IPD) (Weber and Morris model). On the other side, adsorption isotherms were modeled using Langmuir, Freundlich and Temkin models. Adsorption thermodynamics parameters [e.g., Gibbs free

energy (ΔG^o, kJ/mol), enthalpy change (ΔH^o, kJ/mol), entropy change (ΔS^o, J/mol/K)] were determined using Van't Hoff equation.

Regeneration of adsorbent

The reusability of the adsorbent, desorption test, was carried out at 25℃ (pH 2.0, C_o = 10 mg/mL, t = 420 min, and adsorbent dose = 0.05 g) for five consecutive cycles. The acid black II dye bound to the Alg-PAA/f-MWCNTs was exposed to a 25 mL solution with a pH of 12, allowed to reach equilibrium, subjected to filtration, and subsequently analyzed for its dye concentration in the filtrate. After desorption, the Alg-PAA/f-MWCNTs were washed with ultrapure water for the next adsorption cycle.

Results and discussion

Synthesis of the Alg-PAA/f-MWCNTs composite

The overall stepwise synthesis of the Alg-PAA/f-MWCNTs composite is illustrated in **Figure 2** with some modifications of the previously reported protocol.[26, 33, 39] The MWCNTs were functionalized through oxidation steps, creating hydroxyl (-OH) and carboxyl (-COOH) groups as active sites for reacting with the hydroxyl (-OH) groups of the alginate moieties.

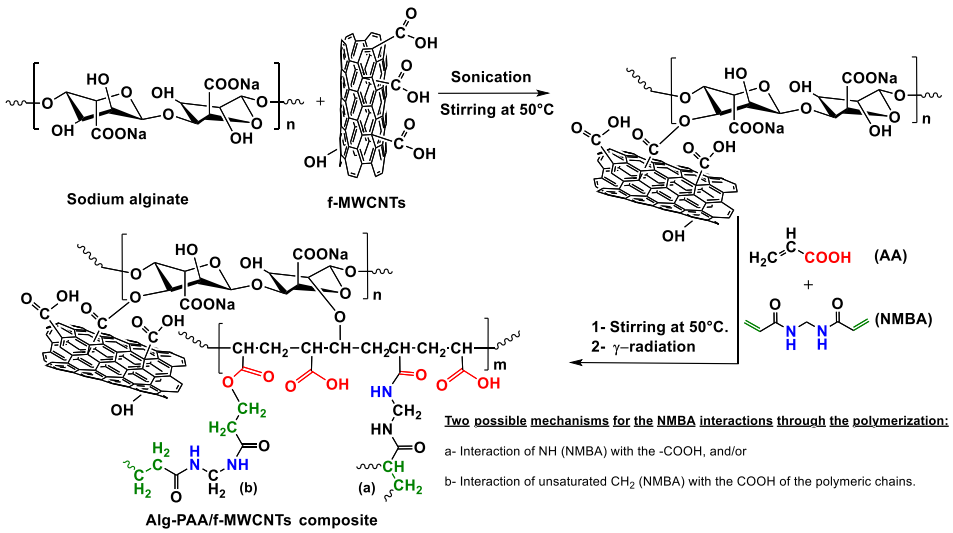

Figure 2. The general strategy for the synthesis of Alg-PAA/f-MWCNTs composite.

Grafting of AA onto the Alg/f-MWCNTs was initiated using γ-radiation by template polymerization technique in the presence of NMBA as a crosslinker. Indeed, two possible mechanisms for the NMBA interactions during polymerization: interaction of the NH group and/or the unsaturated -CH_2 group (NMBA) with the -COOH groups within the polymeric chains.[40] The stepwise synthesis and the proposed structure for the novel Alg-PAA/f-MWCNTs composite is presented in **Figure 2**. The mechanism of grafting AA monomers onto Alg/f-MWCNTs surface by γ-radiation-induced polymerization starts when the high-energy γ-rays interact with AA monomeric units, forming free radicals or other reactive species. This process can be initiated through breaking covalent bonds within AA monomers. The free radicals then react with other AA monomeric units, causing chain propagation, which adds monomers to the growing chain, creating longer chains. The process can terminate through reactions between chains or radical recombination, leading to the end of chain growth. The high energy of γ-rays allows for efficient initiation, and the resulting polymers may exhibit unique properties depending on radiation dose and conditions.[41, 42]

The optimized conditions for yielding the highest grafting percentage, grafting efficiency, and swelling degree were established through studying the influence of the AA, Alg, NMBA (crosslinker), and the f-MWCNTs concentrations.

Optimization conditions for the synthesis of the Alg-PAA/f-MWCNTs composite

Studying the effects of the AA, Alg, NMBA, and f-MWCNTs concentrations on the grafting efficiency (GE%), are the most effective factors in establishing the ideal conditions for the production of the Alg-PAA/f-MWCNTs composite.[43, 44]

Influence of AA concentration

The influence of the AA concentrations on the grafting percentage, grafting efficiency, and swelling degree (S) was studied using a concentration range from 5.0 to 40 wt%, at fixing the concentrations of other parameters (**Figure 3a**). It has been found that G% and GE% were increased while AA concentration increased from 5.0 to 30 wt%, which is associated with the releasing of many free radicals, generating more propagation chains, and the high availability of AA monomers for grafting. The maximum GE% was 85.3 at 30 wt% for AA. The swelling degree was found to be in the range between 1.5 and 4.66.

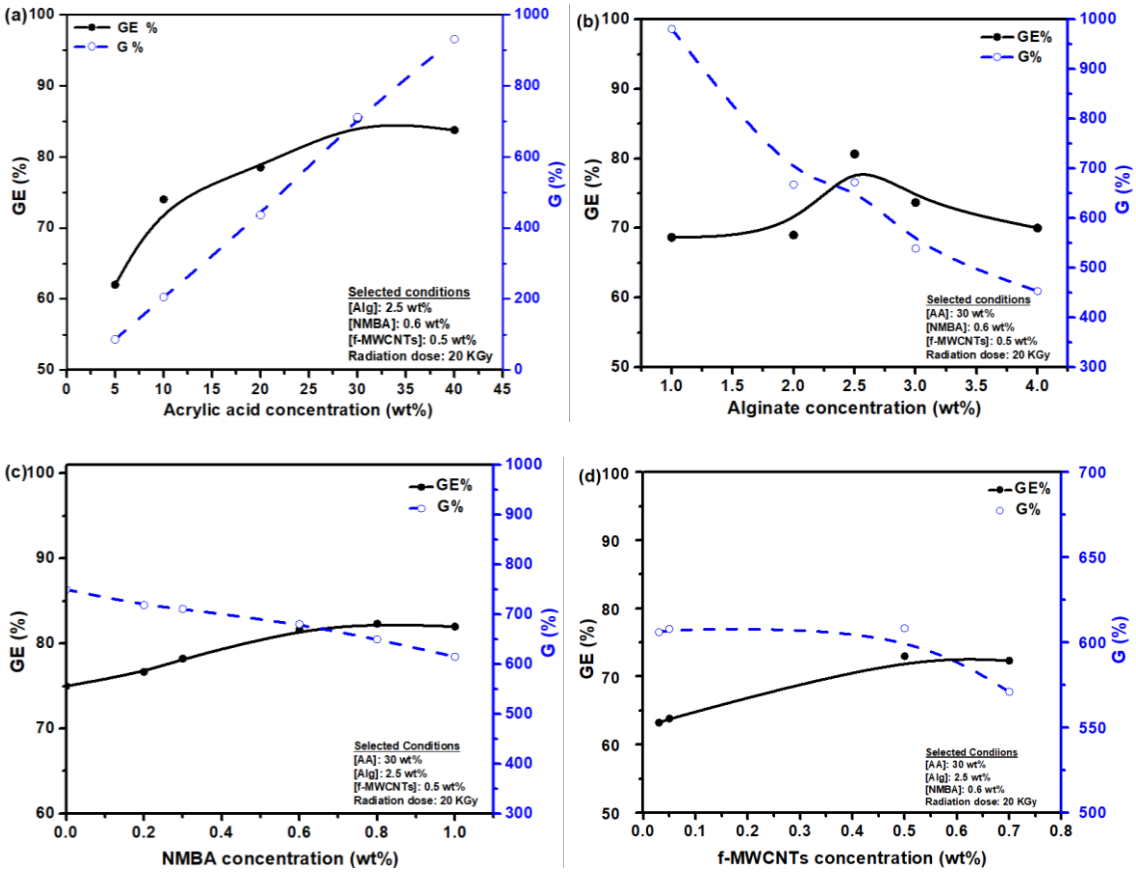

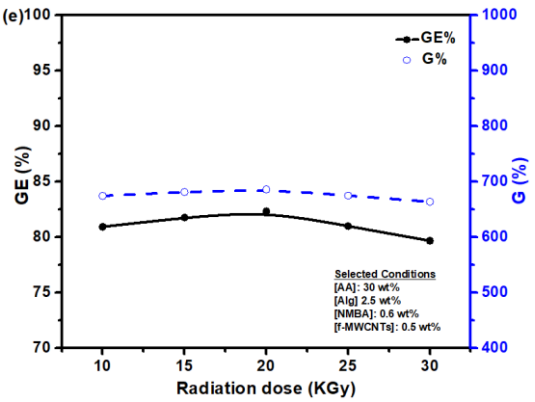

Figure 3. Effect of (a) AA, (b) Alg, (c) NMBA, (d) f-MWCNTs concentrations, and (e) radiation dose on the grafting percentage (G%) and grafting efficiency (GE%).

Influence of alginate concentration

The effect of Alg concentration on the swelling degree, grafting percentageand efficiency was carried out using the Alg concentration range of 1.0 – 4.0 wt% at 30 wt% AA, 0.6 wt% NMBA, 0.5 wt% f-MWCNTs, and a radiation dose of 20 kGy. **Figure 3b** shows that the GE% increased with increasing the Alg concentration from 1.0 to 2.5 wt%. This finding was explained by the availability of more sites for the initiating the polymerization process. Beyond 2.5 wt%, the G% and GE% decreased with increasing the Alg concentration, which was attributed to increasing the reaction medium viscosity, hindering the diffusion of reactive monomers in the system to interact with the growing polymeric chains. Thus, the maximum GE% was 80.6% at 2.5 wt% of Alg concentration, while the swelling degree was found to be from 1.8 to 5.8.

Influence of NMBA concentration

The effect of NMBA concentration on G%, GE%, and the swelling degree was invesitgatd in the NMBA concentration range from 0.0 to 1.0 wt% at the optimized values of other components (2.5 wt% Alg, 30 wt% AA, 0.5 wt% f-MWCNTs and 20 kGy radiation dose) (**Figure 3c**). The G% and GE% increased with increasing the percentage

of crosslinker till 0.6 wt%, which may be due to increasing the free radicals generated from NMBA for generating propagation chains. The decrease in G% was observed while the NMBA concentration exceeded 0.6 wt%, which may be due to a higher extent of the crosslinking between the polymeric chains and NMBA.[45] As a consequence, the probability of monomers' interaction with the added template polymer decreased. The swelling degree was ranged between 0.9 and 4.1.

Influence of f-MWCNTs concentration

The effect of f-MWCNTs concentration on the G%, GE%, and the swelling degree was studied in the concentration range from 0.03 to 0.7 wt%, at the optimized conditions of 2.5 wt% Alg, 30 wt% AA, 0.6 wt% NMBA and 20 kGy radiation dose (**Figure 3d**). The GE% and G% increased with increasing the f-MWCNTs concentration to a maximum values of 0.7 wt% and 0.5 wt% respectively, due to the presence of the active groups (e.g., -OH and -COOH) that act as grafting sites on the f-MWCNTs surface [46]. While a slight decrease in the G% was noticed upon increasing the f-MWCNTs concentration greater than 0.5 wt%, associated with the saturation of active sites. The swelling degree was found to be in the range 3.21 - 6.12.

Influence of radiation dose

The effect of radiation dose on the G%, GE%, and the swelling degree was investigated using the radiation doses from 10 to 30 kGy at 2.5 wt% Alg, 30 wt% AA, 0.6 wt% NMBA, and 0.5 wt% of f-MWCNTs (**Figure 3e**). It was found that G% and GE% slightly increased as the radiation dose increased due to increasing the generated free radicals. The G% and GE% slightly decreased with further increase in the absorbed dose, which may be related to increasing the medium viscosity, hindering the monomers diffusion in

the system.[47] The maximum efficiency (GE%) was 82.33% at a radiation dose of 20 kGy. The swelling degree was found to be from 1.48 to 5.72.

Characterization of the Alg-PAA/f-MWCNTs composite

FTIR, SEM, XRD, TGA and DTA techniques were used to study and validate the structure of the composite. The Zeta potential and point of zero charge of the Alg-PAA/f-MWCNTs composite were also determined.

Fourier-transform infrared analysis

The FTIR spectrum of Alg-AA/f-MWCNTs composite showed the characteristic absorption band of Alg at 1116 cm^{-1}, typically of the stretching vibration of –C–OH (**Figure 4a**).

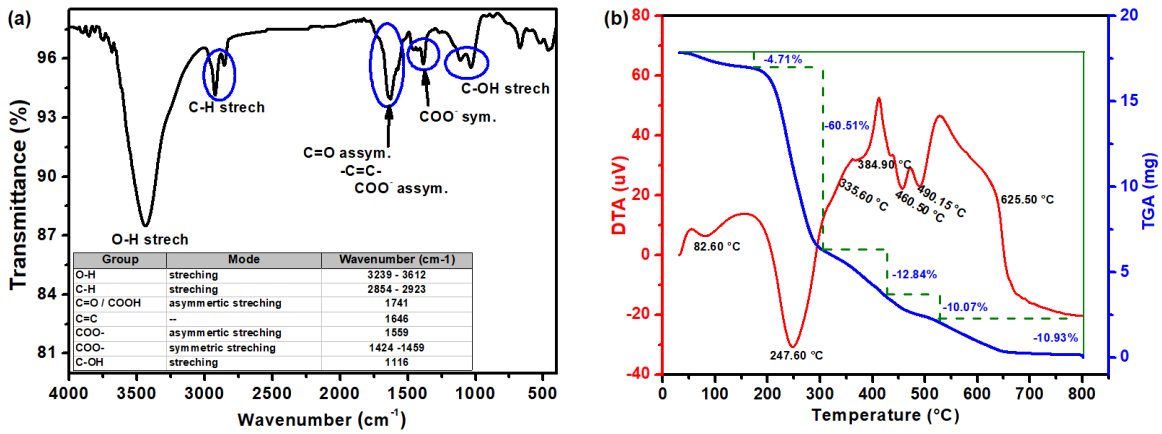

Figure 4. (a) The FTIR spectrum, and (b) TGA and DTA thermograms of Alg-PAA/f-MWCNTs composite.

The bands at 1424 cm^{-1} and 1459 cm^{-1} belong to the symmetric stretching of $–COO^-$ group, while the band at 1559 cm^{-1} was assigned to the asymmetric stretching of $–COO^-$ group of both Alg and AA. The absorption bands at 1741 cm^{-1}, 2854 - 2923 cm^{-1}, and 3239 – 3612 cm^{-1} represented the asymmetric stretching vibration of C=O, –C–H, and –OH groups, respectively of the Alg, AA, and f-MWCNTs. The band at 1646 cm^{-1} denoted

the –C=C– stretching vibration of f-MWCNTs. These findings proved the efficient grafting of the AA onto Alg/f-MWCNTs surface (**Figure 4a**).[48-50]

Thermal analysis

Figure 4b shows the five-stages weight decomposition of Alg-PAA/f-MWCNTs. The first weight loss until temperature of 200^{o}C was found to be 4.7%, corresponding to moisture loss. The second stage demonstrated the highest weight loss of 60.5% between the temperature range 200 - 300^{o}C, which might be associated with the breaking of the main polymer chains. The third step with maximum temperatures at 335^{o}C and 385^{o}C, corresponded to a total weight loss of 12.8% due to decarboxylation of polyacrylic acid (PAA). The fourth stage with maximum temperatures at 460^{o}C and 490^{o}C exhibited a weight loss of 10.1% due to chain fragmentation created by chains' scission. While the last stage occurred at a temperature > 500^{o}C with 10.9% weight loss for the f-MWCNTs decomposition.

X-ray diffraction analysis The XRD pattern of Alg-PAA/f-MWCNTs composite showed broad diffraction spectrum (**Figure S1; Supporting data**). It is known that Alg and PAA have amorphous nature, while the f-MWCNTs exhibit two characteristic diffraction peaks at 2θ values of approximately 26.0° and 43.9°, corresponding to the (002) and (100) reflections, respectively.[51] In this study, the XRD spectrum of Alg-PAA/f-MWCNTs composite revealed three main humps at 2θ = 20.15°, 31.23°, and 42.86°. The amorphous nature of the Alg-PAA/f-MWCNTs was attributed to the non-crystalline character induced by both Alg and PAA.[52] The broad hump at 2θ = 20.15° may be related to grafting of AA onto Alg/f-MWCNTs and destruction of the crystallinity, while the two humps belong to the f-MWCNTs at 2θ = 31.23°, and 42.86° showed slight shift from the reported values, suggesting strong ionic interactions between the components of Alg-PAA/f-MWCNTs composite.[53]

Particle size analysis

Particle size and size distribution are important parameters for evaluating physical stability, homogeneity, and the sedimentation rate of the nanoparticle suspension. The particle size distribution of Alg-PAA/MWCNTs was measured through the polydispersity Index (PDI) using DLS-Malvern Zeta sizer. The analysis showed a PDI value of 1.00 for Alg-AA/MWCNTs, and the composite mostly has a uniform particles size of 150.7 nm (**Figure S2; Supporting data**). This uniform distribution and small particles of Alg-PAA/MWCNTs composite enable a larger surface area exposure for adsorption.[54]

Point of zero charge and Zeta potential analyiss

Zeta potential measurements are conducted to provide information about the surface charge of Alg-PAA/f-MWCNTs composite. It has been reported that the pH_{pzc} of pristine MWCNTs occurs at pH = 3.7, and the Zeta potential values are positive at pH < pH_{pzc}.[55] In the current study, the findings revealed that the isoelectric point (pH_{pzc}) of the composite occurs at pH = 6.28 (**Figure S3a; Supporting data**). On the other hand, the Zeta potential values of Alg-PAA/f-MWCNTs composite are negative (-12.00 to -30.2 mV) in the whole pH range, and the potentials become more negative as pH increases from 2.0 to 12.0 (**Figure S3b; Supporting data**). The negative potentials agree with previously reported values for functionalized-MWCNTs due to the added Alg and PAA to the f-MWCNTs surface.[55] These findings interpret the highest removal of the anionic nigrosine dye by Alg-PAA/f-MWCNTs at pH < pH_{pzc} reaching a maximum at pH = 2.0. At pH values < pH_{pzc} there is an elevation in the concentration of H^+ ions in the solution. Consequently, the Alg-PAA/f-MWCNTs surface becomes protonated in an acidic environment, leading to the formation of robust electrostatic forces of attraction between the anionic nigrosine dye and function groups (e.g., -COOH, -OH) existing on the adsorbent Alg-PAA/f-MWCNTs surface.[56]

Scanning electron microscopy

The microstructure morphology and homogeneity of the Alg-PAA/f-MWCNTs composite were inspected through the SEM analysis was done to inspect (**Figure 5**). The SEM micrograph (**Figure 5b**) demonstrated a uniform and homogeneous of entangled multilayered texture exhibiting holes with nearly equal radii distributed on the surface compared with the micrograph of the Alg polymer (**Figure 5a**). These large continuous interconnected layers create active sites which could increase the adsorption ability of the dyes onto the composite's surface.

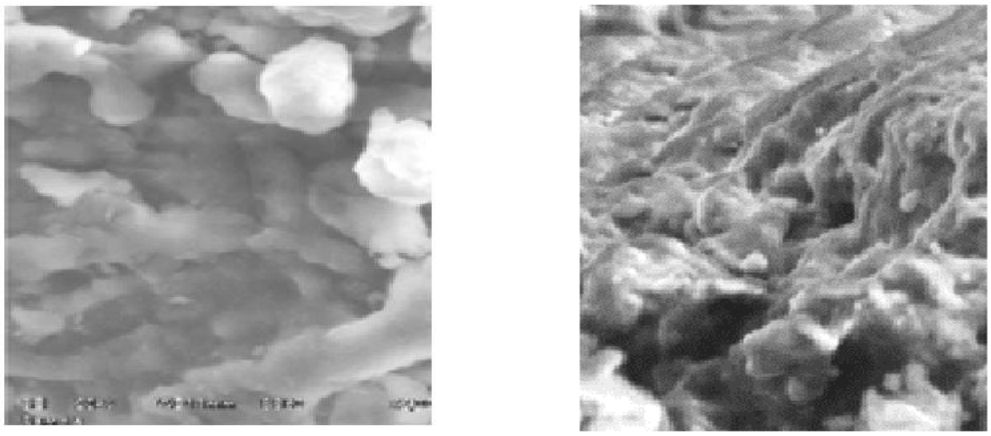

Figure 5. SEM micrographs of (a) Alg polymer and (b) Alg-PAA/f-MWCNTs composite.

Adsorption performance of Alg-PAA/f-MWCNTs

Initial pH effect

The removal of dye from aqueous solutions is highly pH dependent. A variation in pH can influence the interactions between dye and adsorbents molecules due to the change in the ionization level and surface charge of the absorbent. As a result, the impact of the initial pH of the solutions on acid black II dye removal was investigated over a pH range of (2.0 – 12.0) (**Figure 6a**). The data investigated that the maximum dye removal of 83.0% was observed at pH 2.0, then a significant decrease in dye removal was observed

by increasing the pH of the medium. The removal % was reduced significantly from 32.0% at pH 3 reaching to 0% at pH 12, associated with increasing the electrostatic repulsion.

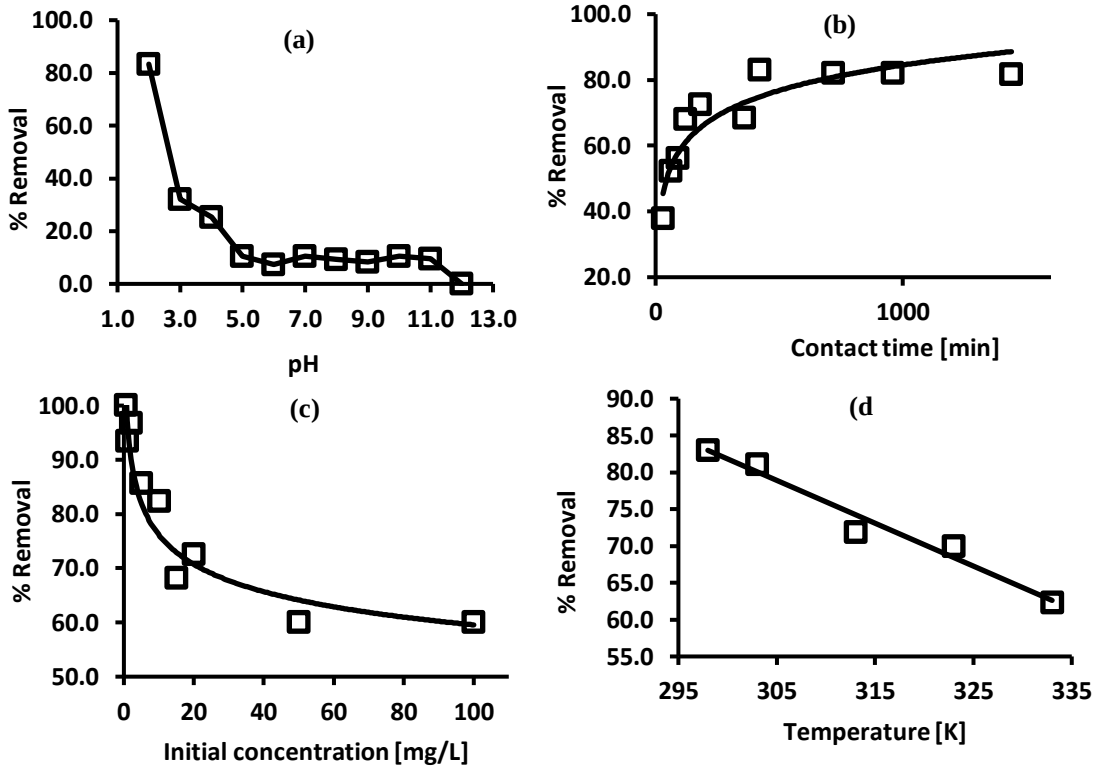

Figure 6. Effect of (a) pH, (b) contact time, (c) initial dye concentration, and (d) temperature on the % removal of acid black II by Alg-PAA/f-MWCNTs adsorbent.

It has been reported that in an aqueous solution, acidic dye dissolves first, then dissociates, resulting in anionic dye ions.[18, 57] At low pH most of the functional groups on the adsorbent surface such as –OH, –COOH, were protonated led to a significant electrostatic attraction for the anionic acid black II dye.[58, 59] As the pH increases, the adsorption capacity decreased, which could be attributed to an increase in the number of negatively charged sites on the adsorbent surface, and hence a decrease in electrostatic attraction and competition for adsorption between acid black II dye and OH^- ions. In the current study, the pH value of 2.0 was selected as the optimum pH and used in the next

experiments with maximum removal of 83.0%. This finding matches with the observed point of zero charge of the composite at pH_{pzc} = 6.28 (**Figure S3; Supporting data**), below which the dye removal increases reaching the maximum at pH = 2.0 (**Figure 6a**).

Effect of contact time

Time of contact is a crucial parameter of consideration when designing a low-cost wastewater treatment system [60]. The effect of contact time (30 – 1440 min) on the adsorption was studied at the optimum pH conditions for the Alg-PAA/f-MWCNTs composite. The results presented in **Figure 6b**, showed an optimum equilibrium time of 420 min was sufficient to attain equilibrium for adsorption of acid Back II onto Alg-PAA/f-MWCNTs composite with the removal of 83.0% and maximum loading capacity of 4.15 mg/g.

Effect of initial dye concentration

The influence of acid black II dye concentrations was investigated using the concentration range 0.5 - 100 mg/L (**Figure 6c**). The highest removal (> 99.0%) was observed at lower dye concentration (0.5-10 mg/L) may be attributed to the low (dye ion/binding sites) ratio. As the concentration of dye increased, the adsorption ability decreased since all active sites and the internal pores become saturated.[61, 62]

Influence of temperature

The temperature has a significant effect on the adsorption mechanism because temperature variations induce various changes in the adsorbent's equilibrium potential for the adsorption of a certain adsorbate.[63] Adsorption tests on Alg-PAA/f-MWCNTs nanocomposite polymer were carried out at different temperatures (293, 303, 313, 323, and 333 K), **Figure 6d**. The results indicated that the removal% of acid black II dye by

Alg-PAA/f-MWCNTs declined with increasing the temperature which highlights exothermic adsorption.

Adsorption kinetics, isotherm, and thermodynamics

Adsorption kinetics studies

The mechanism and rate of the adsorption process can be predicted based on kinetics studies. Sorption kinetics of dye on the solid surface is usually explained as: the mass transfer step when the dye molecules are rapidly transferred from the bulk solution to the adsorbent surface, and a diffusion step in which dye molecules diffuse from the boundary film of the sorbent into the inner active sites. The rate of diffusion step and dye adsorption (K_{id}) is lower than the first step due to an increase in boundary layer film and a decrease in vacant active sites accompanying the complexation, physicochemical sorption or ion exchange processes. In the present study, the kinetics of adsorption were studied using pseudo-first order, pseudo-second, and intra-particle diffusion models. For the adsorption of acid back II on Alg-PAA/f-MWCNTs composite, the validity of the pseudo-first order (Eq. 5), pseudo-second order (Eq. 6), and diffusion kinetics using Weber and Morris intra-particle diffusion (Eq. 7) models, were checked.[37] The perfectly suited model was chosen according to the limit of compatibility between the calculated and experimental (Q_e) values, as well as the linear correlation coefficient values (R^2).

$$\ln(Q_e - Q_t) = \ln Q_e - k_1 t \qquad (Eq.\ 5)$$

$$\frac{t}{Q_t} = \frac{1}{k_2 Q_e^2} + \frac{t}{Q_e} \qquad (Eq.\ 6)$$

$$Q_t = K_{id} t^{0.5} + C \qquad (Eq.\ 7)$$

Where, Q_e and Q_t are the adsorption capacity (mg/g) of adsorbents at equilibrium and at time t (min), respectively. The k_1 (min^{-1}) and k_2 (g/mg/min) are the pseudo-first order and pseudo-second order rate constant values, respectively. The K_{id} ($mg/g/min^{1/2}$) is the intra-particle diffusion coefficient and C is the thickness of the boundary layer. The various

parameters were calculated by linear fitting the three models as shown in **Figures 7a-c** and **Table 1**.

Table 1. Kinetic parameters for the sorption of acid black II on Alg-PAA/f-MWCNTs

	Pseudo-first order			**Pseudo-second order**				**Intra-particle diffusion**		
Q_e(Exp.)	k_1	Q_e(Cal.)	R^2	k_2	Q_e(Cal.)	h	R^2	K_{id}	C	R^2
mg/g	min^{-1}	mg/g		g/mg/min	mg/g	$k_2 Q_e^2$		$mg/g/min^{1/2}$	-	
4.12	0.0023	1.78	0.577	0.0079	**4.24**	0.0936	**0.999**	0.0872	1.6592	0.714

Pseudo-second order has the highest R^2 (0.999) compared to other adsorption kinetic models, suggesting that the adsorption behaviour occurs mainly on the surface of Alg-PAA/f-MWCNTs, and controlled by the chemisorption mechanism (**Figure 7b**). The rate-limiting step is controlled by sharing or exchanging of electrons between the dye molecule and the adsorbate.

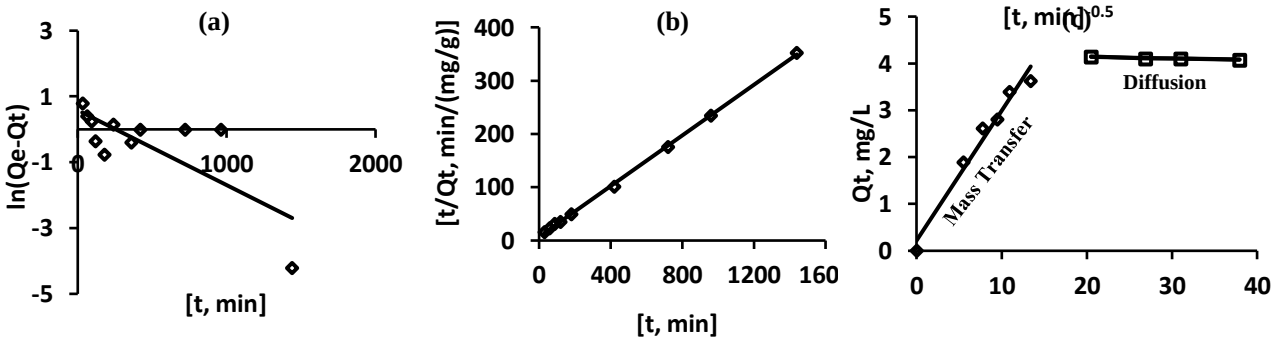

Figure 7. Kinetic plots for the sorption of acid black II over Alg-PAA/f-MWCNTs, (a) pseudo-first order model, (b) pseudo-second order, and (c) intra-particle diffusion models.

The calculated equilibrium adsorption capacity (Q_e) from pseudo-second order has values of 4.12 mg/g for acid black II sorption onto Alg-PAA/f-MWCNTs composite which are very close to the experimental values of 4.24 mg/g ($\Delta q = 0.12$). The pseudo-second order

rate constant (k_2**)** indicated that the adsorption process was achieved very fast. The intra-particle diffusion model (**Figure 7c**) showed two linear sections plots; thus the model cannot be accepted as the only rate-determining step. The first linear part in the model represents the mass transfer from solution to the solid surface (R^2 = 0.971) while the second part shows the diffusion of dye molecules from the surface to the inner layer (R^2 = 0.808).

Adsorption isotherms studies

Three isotherm models were applied for studying the adsorption of acid black II on Alg-PAA/f-MWCNTs namely Freundlich (Eq. 8) [64], Langmuir (Eq. 9) [65], and Temkin (Eq. 10) [66] models.

$$Q_e = K_F C_e^{1/n} \qquad \ln Q_e = \ln K_F + \frac{1}{n}\ln C_e \qquad \text{(Eq. 8)}$$

$$\frac{1}{Q_e} = \frac{1}{bQ_m}\frac{1}{C_e} + \frac{1}{Q_m} \qquad Q_e = \frac{Q_m\, bC_e}{1 + bC_e} \qquad \text{(Eq. 9)}$$

$$Q_e = B_T(\ln K_T) + B_T(\ln C_e) \qquad B_T = (RT)/b \qquad \text{(Eq. 10)}$$

B_T is Temkin constant = RT/b (J/mol) and related to the heat of adsorption, while T is the absolute temperature (K); R is the ideal gas constant = 8.314 J/mol/K, and K_T is the equilibrium binding constant (L/min) related to the higher binding energy.

The adsorption of acid black II on Alg-PAA/f-MWCNTs has the highest R^2 (0.9601) with the Freundlich model compared to Langmuir (R^2 = 0.816), and Temkin (R^2 = 0.625), (**Figures 8a-c**) and (**Table 2**). This indicates that the adsorption mechanism is well fitting with the Freundlich isotherm model and the adsorption of acid black II on Alg-PAA/f-MWCNTs is closer to multi-layer adsorption with multiple adsorption sites (**Figure 8a**). The value of the Freundlich isotherm $0 < 1/n = 0.569 < 1$), indicating that the interaction between Alg-PAA/f-MWCNTs and dye molecules is strong, and the sorption process is likely to be favourable (**Table 2**).

Table 2. Isotherm parameters for the sorption of acid black II onto Alg-PAA/f-MWCNTs

Freundlich		Langmuir		Temkin	
n	1.757	Q_m	6.69	B_T	742.7
1/n	0.5691	b	1.7589	K_T	6.505
K_F	11.633				
R^2	0.9601	R^2	0.8164	R^2	0.6256

Figure 8. Isotherm plots for the sorption of acid black II on Alg-PAA/f-MWCNTs using

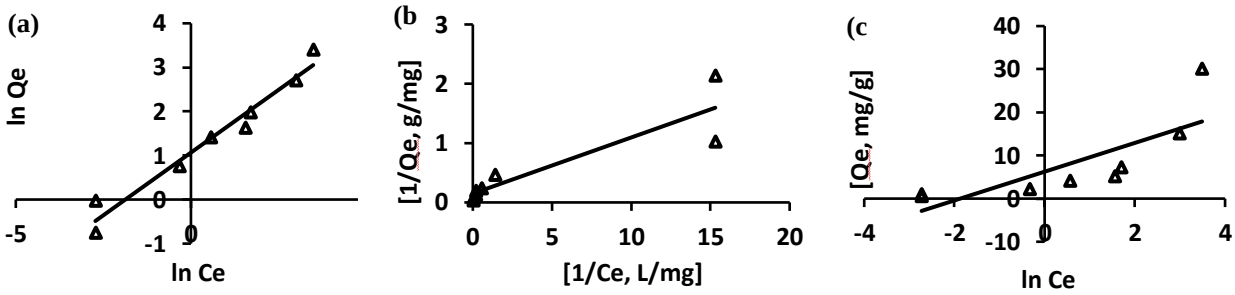

(a) Freundlich, (b) Langmuir, and (c) Temkin models.

However, the R^2 of Alg-PAA/f-MWCNTs for acid black II sorption using Langmuir model close to 0.816, it was not fit with the known features of removal rate (i.e., high removal at low concentration and low removal at high concentration), (**Figure 8b**) and (**Table 2**). This principle could be achieved using Freundlich model, the theoretical adsorption capacity increased with increasing the initial concentration of the dye solution. Thus, proved that the Freundlich adsorption model was more fitting for the adsorption of acid black II on Alg-PAA/f-MWCNTs.

Thermodynamic studies

Thermodynamic parameters including the changes in Gibbs free energy (ΔG^o, kJ/mol), enthalpy change (ΔH^o, kJ/mol), and entropy change (ΔS^o, J/mol/K) were calculated from the following equations (11 - 14).

$$\ln K_d = \frac{\Delta S^0}{R} - \frac{\Delta H^0}{RT} \qquad \text{(Eq. 11)}$$

$$K_d = \frac{Q_e}{C_e} \quad \text{(Eq. 12)}$$

$$\Delta G^0 = \Delta H^0 - T\Delta S^0 \quad \text{(Eq. 13)}$$

$$\Delta G^0 = -RT \ln K_d \quad \text{(Eq. 14)}$$

Where R (8.314 J/mol/K) is the universal gas constant, T (K) is the absolute temperature and K_d is the distribution coefficient. The Linear plot of ln K_d *versus* 1/T for adsorption gives the slope and intercept equal to ($-\Delta H^o/R$) and ($\Delta S^o/R$), respectively. Indeed, the negative value of ΔG^o confirmed the spontaneous nature and possibility of the adsorption *via* physical force. The results are summarized in **Table 3** and **Figure 9**. The sorption was random and thermodynamically favourable, as shown by the negative ΔG^o values. Extra negative ΔG^o indicated a stronger adsorption driving force, resulting in a higher sorption power. Furthermore, the negative value of the entropy (ΔS^o = -78.76) implied the decrease in the system's degree of freedom. The negative ΔH^o value of (-17.850) in the case of acid black II sorption suggested exothermic adsorption.[37]

Table 3. Thermodynamics parameters for acid black II adsorption on Alg-PAA/f-MWCNTs

T K	ΔG^o (kJ/mol)	ΔH^o (kJ/mol)	ΔS^o (J/mol/K)
303	-2.0211		
313	-0.6447	-25.699	-78.76
323	-0.4682		
332	0.5284		

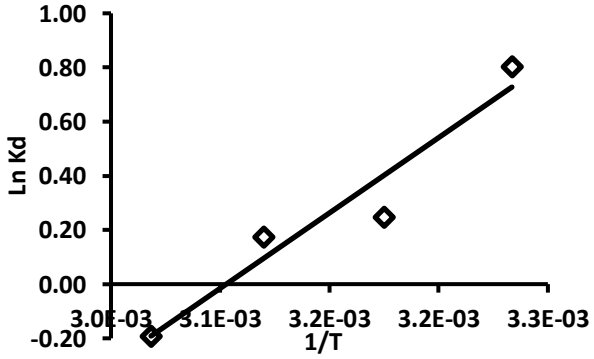

Figure 9. Thermodynamic plot for acid black II adsorption on Alg-PAA/f-MWCNTs composite.

Reusability of Alg-PAA/f-MWCNTs composite

To evaluate the reusability of Alg-PAA/f-MWCNTs composite as adsorbent, five sequential adsorption-desorption cycles were performed at the optimal conditions where the adsorbed dye was rapidly desorbed in an alkaline medium. The effect of five reused cycles on the adsorption capacity of Alg-PAA/f-MWCNTs (**Figure S4; Supporting data**). It could be deduced that the adsorption capacity of Alg-PAA/f-MWCNTs composite was above 80% after five-consecutive adsorption–desorption processes, provoking the high-performance recyclability of the Alg-PAA/f-MWCNTs composite on acid black II dye removal.

Comparison of the acid black II adsorption capacities of Alg-PAA/f-MWCNTs adsorbent with other previously studied adsorbents is listed in **Table S1** (**Supporting data**). Based on the results, the Alg-PAA/f-MWCNTs adsorbent is regarded as a promising adsorbent and a good candidate for the removal of acid black II from wastewater.

The study concludes that an alginate-polyacrylic acid/multiwalled carbon nanotubes (Alg-PAA/f-MWCNTs) composite was successfully prepared *via* gamma radiation-induced template polymerization of AA onto Alg/f-MWCNTs surface. The maximum grafting efficiency (GE%) of ~ 82% was obtained under optimized conditions of 2.5 wt% Alg, 30 wt% AA, 0.5 wt% f-MWCNTs, 0.6 wt% *N*,*N*′-methylenebisacrylamide (NMBA), and irradiation dose ~ 20 kGy. The structure and thermal characteristics of the prepared composite were validated by FTIR, SEM, TGA, XRD, and DTA. The Alg-PAA/f-MWCNTs composite exhibited uniform small particles size, with negative Zeta potentials within the whole pH range of a minimum at pH = 2. The adsorption batch experiments showed good adsorption capacity in the removal of the nigrosine dye from an aqueous medium with adsorption efficiency of 83% . Adsorption of nigrosine dye onto the

620 composite was favourable thermodynamically obeying the Freundlich isotherm model
621 and controlled by chemisorption mechanism Interestingly, the composite showed a good
622 regeneration ability in the removal of the dye several times under the optimized
623 conditions. Accordingly, the Alg-PAA/f-MWCNTs composite could be a promising
624 candidate for the treatment of wastewaters from nigrosine dye.

625 **Acknowledgments**

626 This research did not receive any specific grant from funding agencies in the public,
627 commercial, or not-for-profit sectors. Authors acknowledge the National Institute of
628 Oceanography and Fisheries (NIOF, Egypt), and the Hot Labs Center (Nuclear Chemistry
629 Department, Uranium Products Pilot Plant (UPPP), Second Research Reactor (ETRR-2)
630 and Labeled Compounds Department of Egyptian Atomic Energy Authority, for the
631 fruitful collaboration through their scientific and technical facilities.

632

633 **Declaration of interest statement**

634 **Conflict of interest:** The authors report there are no competing interests to declare.

635 **Funding:** The authors did not receive support from any organization for the submitted
636 work.

637

638 **Author contributions: Mohamed I. A. Ibrahim:** Conceptualization, Methodology,
639 Methods validation, Data curation and analysis, Writing and Reviewing. **Islam M.**
640 **Abdelmonem:** Conceptualization, Methodology, Data analysis, and Reviewing. **Laila.**
641 **A. Mohamed:** Conceptualization, Methodology, Methods validation, Data curation and
642 analysis, Writing and Reviewing. **Mohamed A. Gizawy:** Conceptualization,
643 Methodology, Data analysis and Reviewing. **Essam Metwally:** Conceptualization and
644 Reviewing.

645

646

References

1. Yagub, M. T.; Sen, T. K.; Afroze, S.; Ang, H. M., Dye and its removal from aqueous solution by adsorption: a review. *Advances in colloid and interface science* 2014, *209*, 172-84.https://doi.org/10.1016/j.cis.2014.04.002
2. Brillas, E.; Martínez-Huitle, C. A., Decontamination of wastewaters containing synthetic organic dyes by electrochemical methods. An updated review. *Applied Catalysis B: Environmental* 2015, *166-167*, 603-643.https://doi.org/10.1016/j.apcatb.2014.11.016
3. Nirmaladevi, S.; Palanisamy, N., A comparative study of the removal of cationic and anionic dyes from aqueous solutions using biochar as an adsorbent. *Desalination and Water Treatment* 2020, *175*, 282-292.https://doi.org/10.5004/dwt.2020.24906
4. Yusuf, M., Synthetic Dyes: A Threat to the Environment and Water Ecosystem. 2019, 11-26.https://doi.org/10.1002/9781119526599.ch2
5. Dotto, J.; Fagundes-Klen, M. R.; Veit, M. T.; Palácio, S. M.; Bergamasco, R., Performance of different coagulants in the coagulation/flocculation process of textile wastewater. *Journal of Cleaner Production* 2019, *208*, 656-665.https://doi.org/10.1016/j.jclepro.2018.10.112
6. Sh. Gohr, M.; Abd-Elhamid, A. I.; El-Shanshory, A. A.; Soliman, H. M. A., Adsorption of cationic dyes onto chemically modified activated carbon: Kinetics and thermodynamic study. *Journal of Molecular Liquids* 2022, *346*, 118227.https://doi.org/10.1016/j.molliq.2021.118227
7. Cinperi, N. C.; Ozturk, E.; Yigit, N. O.; Kitis, M., Treatment of woolen textile wastewater using membrane bioreactor, nanofiltration and reverse osmosis for reuse in production processes. *Journal of Cleaner Production* 2019, *223*, 837-848.https://doi.org/10.1016/j.jclepro.2019.03.166
8. Punzi, M.; Nilsson, F.; Anbalagan, A.; Svensson, B. M.; Jönsson, K.; Mattiasson, B.; Jonstrup, M., Combined anaerobic-ozonation process for treatment of textile wastewater: removal of acute toxicity and mutagenicity. *Journal of hazardous materials* 2015, *292*, 52-60.https://doi.org/10.1016/j.jhazmat.2015.03.018
9. Wang, C.-C.; Li, J.-R.; Lv, X.-L.; Zhang, Y.-Q.; Guo, G., Photocatalytic organic pollutants degradation in metal–organic frameworks. *Energy & Environmental Science* 2014, *7* (9), 2831-2867.https://doi.org/10.1039/C4EE01299B
10. Jaafar, M. T., UV-A Activated ZnO Mediated Photocatalytic Decolorization of Nigrosine (Acid Black 2) Dye in Aqueous Solution. *Journal of Geoscience and Environment Protection* 2017, *5* (9), 1-10.https://doi.org/10.4236/gep.2017.59010
11. Sözen, S.; Olmez-Hanci, T. b.; Hooshmand, M.; Orhon, D. J. E. C. L., Fenton oxidation for effective removal of color and organic matter from denim cotton wastewater without biological treatment. 2019, *18*, 207-213.https://doi.org/10.1007/s10311-019-00923-8
12. Jedynak, K.; Wideł, D.; Rędzia, N., Removal of Rhodamine B (A Basic Dye) and Acid Yellow 17 (An Acidic Dye) from Aqueous Solutions by Ordered Mesoporous Carbon and Commercial Activated Carbon. 2019, *3* (1), 30.https://doi.org/10.3390/colloids3010030

13. Ghanavati Nasab, S.; Semnani, A.; Teimouri, A.; Kahkesh, H.; Momeni Isfahani, T.; Habibollahi, S., Removal of Congo Red from Aqueous Solution by Hydroxyapatite Nanoparticles Loaded on Zein as an Efficient and Green Adsorbent: Response Surface Methodology and Artificial Neural Network-Genetic Algorithm. *Journal of Polymers and the Environment* 2018, *26* (9).https://doi.org/10.1007/s10924-018-1246-z
14. He, K.; Zeng, G.; Chen, A.; Huang, Z.; Peng, M.; Huang, T.; Chen, G., Graphene hybridized polydopamine-kaolin composite as effective adsorbent for methylene blue removal. *Composites Part B: Engineering* 2019, *161*, 141-149.https://doi.org/10.1016/j.compositesb.2018.10.063
15. Robati, D.; Mirza, B.; Rajabi, M.; Moradi, O.; Tyagi, I.; Agarwal, S.; Gupta, V. K., Removal of hazardous dyes-BR 12 and methyl orange using graphene oxide as an adsorbent from aqueous phase. *Chem. Eng. J.* 2016, *284*, 687-697.https://doi.org/10.1016/j.cej.2015.08.131
16. Zhang, F.; Ma, B.; Jiang, X.; Ji, Y., Dual function magnetic hydroxyapatite nanopowder for removal of malachite green and Congo red from aqueous solution. *Powder Technology* 2016, *302*, 207-214.https://doi.org/10.1016/j.powtec.2016.08.044
17. Ishak, S. A.; Murshed, M. F.; Md Akil, H.; Ismail, N.; Md Rasib, S. Z.; Al-Gheethi, A. A. S., The Application of Modified Natural Polymers in Toxicant Dye Compounds Wastewater: A Review. 2020, *12* (7), 2032.https://doi.org/10.3390/w12072032
18. Zhou, Y.; Lu, J.; Zhou, Y.; Liu, Y., Recent advances for dyes removal using novel adsorbents: A review. *Environmental pollution (Barking, Essex : 1987)* 2019, *252* (Pt A), 352-365.https://doi.org/10.1016/j.envpol.2019.05.072
19. Pino-Ramos, V. H.; Ramos-Ballesteros, A.; López-Saucedo, F.; López-Barriguete, J. E.; Varca, G. H. C.; Bucio, E., Radiation Grafting for the Functionalization and Development of Smart Polymeric Materials. *Topics in current chemistry (Cham)* 2016, *374* (5), 63.10.1007/s41061-016-0063-x
20. Samuel, A. H.; Magee, J. L., Theory of Radiation Chemistry. II. Track Effects in Radiolysis of Water. *The Journal of Chemical Physics* 2004, *21* (6), 1080-1087.10.1063/1.1699113 %J The Journal of Chemical Physics
21. Nasef, M. M.; Gürsel, S. A.; Karabelli, D.; Güven, O., Radiation-grafted materials for energy conversion and energy storage applications. *Progress in Polymer Science* 2016, *63*, 1-41.https://doi.org/10.1016/j.progpolymsci.2016.05.002
22. Bhattacharya, A.; Misra, B. N., Grafting: a versatile means to modify polymers: Techniques, factors and applications. *Progress in Polymer Science* 2004, *29* (8), 767-814.https://doi.org/10.1016/j.progpolymsci.2004.05.002
23. Schulze, A.; Marquardt, B.; Kaczmarek, S.; Schubert, R.; Prager, A.; Buchmeiser, M. R., Electron Beam-Based Functionalization of Poly(ethersulfone) Membranes. 2010, *31* (5), 467-472.https://doi.org/10.1002/marc.200900666
24. Al-Gahtany, S. A., Effect of Polyvinyl Alcohol (PVA) Molecular Weight on the Characteristics of Radiation Synthesized p(AAc/PVA/PEO) Hydrogel Membranes. *Middle East Journal of Applied Sciences* 2024, *14* (1), 43-56.10.36632/mejas/2024.14.1.4

25. Gombotz, W. R.; Wee, S. F., Protein release from alginate matrices. *Advanced Drug Delivery Reviews* 2012, *64*, 194-205.https://doi.org/10.1016/j.addr.2012.09.007
26. Gizawy, M. A.; Shamsel-Din, H. A.; Abdelmonem, I. M.; Ibrahim, M. I. A.; Mohamed, L. A.; Metwally, E., Synthesis of chitosan-acrylic acid/multiwalled carbon nanotubes composite for theranostic 47Sc separation from neutron irradiated titanium target. *International Journal of Biological Macromolecules* 2020, *163*, 79-86.https://doi.org/10.1016/j.ijbiomac.2020.06.249
27. Dubey, R.; Dutta, D.; Sarkar, A.; Chattopadhyay, P., Functionalized carbon nanotubes: synthesis, properties and applications in water purification, drug delivery, and material and biomedical sciences. *Nanoscale Advances* 2021, *3* (20), 5722-5744.10.1039/D1NA00293G
28. Benhouria, A.; Islam, M. A.; Zaghouane-Boudiaf, H.; Boutahala, M.; Hameed, B. H., Calcium alginate–bentonite–activated carbon composite beads as highly effective adsorbent for methylene blue. *Chem. Eng. J.* 2015, *270*, 621-630.https://doi.org/10.1016/j.cej.2015.02.030
29. Fan, J.; Shi, Z.; Lian, M.; Li, H.; Yin, J., Mechanically strong graphene oxide/sodium alginate/polyacrylamide nanocomposite hydrogel with improved dye adsorption capacity. *Journal of Materials Chemistry A* 2013, *1* (25), 7433-7443.10.1039/C3TA10639J
30. Sui, K.; Li, Y.; Liu, R.; Zhang, Y.; Zhao, X.; Liang, H.; Xia, Y., Biocomposite fiber of calcium alginate/multi-walled carbon nanotubes with enhanced adsorption properties for ionic dyes. *Carbohydrate Polymers* 2012, *90* (1), 399-406.https://doi.org/10.1016/j.carbpol.2012.05.057
31. Wang, Y.; Wang, W.; Wang, A., Efficient adsorption of methylene blue on an alginate-based nanocomposite hydrogel enhanced by organo-illite/smectite clay. *Chem. Eng. J.* 2013, *228*, 132-139.https://doi.org/10.1016/j.cej.2013.04.090
32. Clark, G., Staining Procedures Used by the Biological Stain Commission. 4th Edition, Williams & Wilkins, Baltimore, London, 412. 1981,
33. Abdelmonem, I. M.; Metwally, E.; Siyam, T. E.; El-Nour, F. A.; Mousa, A. R. M., Radiation synthesis of starch-acrylic acid–vinyl sulfonic acid/multiwalled carbon nanotubes composite for the removal of 134 Cs and 152+ 154 Eu from aqueous solutions. *Journal of Radioanalytical and Nuclear Chemistry* 2019, *319* (3), 1145-1157. https://doi.org/10.1007/s10967-018-6392-1
34. El-sigeny, S., Preparation and Characterization of Hydrogel based on Chitosan for Removal of Heavy Metal Ions. *International Journal of Advanced Research* 2015, *3* (1), 963-976.Corpus ID: 138469675
35. Mishra, M. M.; Sand, A.; Mishra, D. K.; Yadav, M.; Behari, K., Free radical graft copolymerization of N-vinyl-2-pyrrolidone onto k-carrageenan in aqueous media and applications. *Carbohydrate Polymers* 2010, *82* (2), 424-431. https://doi.org/10.1016/j.carbpol.2010.04.080
36. Saleem, H., Exploitation of Low Cost Coal Fly Ash Adsorbent with Coagulants for the Treatment of Industrial Complex Nature Dyes Wastewater. *International Journal of Scientific and Engineering Research* 2013.Corpus ID: 18389333

776 37. Heiba, H. F.; Taha, A. A.; Mostafa, A. R.; Mohamed, L. A.; Fahmy, M. A.,
777 Preparation and characterization of novel mesoporous chitin blended MoO3-
778 montmorillonite nanocomposite for Cu(II) and Pb(II) immobilization. *International*
779 *Journal of Biological Macromolecules* 2020, *152*, 554-
780 566.https://doi.org/10.1016/j.ijbiomac.2020.02.254
781 38. Khalil, T. E.; Elhusseiny, A. F.; El-dissouky, A.; Ibrahim, N. M., Functionalized
782 chitosan nanocomposites for removal of toxic Cr (VI) from aqueous solution. *Reactive*
783 *and Functional Polymers* 2020, *146*,
784 104407.https://doi.org/10.1016/j.reactfunctpolym.2019.104407
785 39. Abdelmonem, I. M.; Metwally, E.; Siyam, T. E.; El-Nour, F. A.; Mousa, A.-R.
786 M., Adsorption of 60Co from aqueous solution onto alginate–acrylic acid–vinylsulfonic
787 acid/multiwalled carbon nanotubes composite. *Polymer Bulletin* 2020, *77* (9), 4631-
788 4653.10.1007/s00289-019-02978-7
789 40. Abdelmonem, I. M.; Metwally, E.; Siyam, T. E.; El-Nour, F. A.; Mousa, A.-R.
790 M., Radiation synthesis of starch-acrylic acid–vinyl sulfonic acid/multiwalled carbon
791 nanotubes composite for the removal of 134Cs and 152+154Eu from aqueous solutions.
792 *Journal of Radioanalytical and Nuclear Chemistry* 2019, *319* (3), 1145-
793 1157.10.1007/s10967-018-6392-1
794 41. Ashfaq, A.; Clochard, M. C.; Coqueret, X.; Dispenza, C.; Driscoll, M. S.;
795 Ulański, P.; Al-Sheikhly, M., Polymerization Reactions and Modifications of Polymers
796 by Ionizing Radiation. *Polymers* 2020, *12* (12).10.3390/polym12122877
797 42. Ferry, M.; Ngono-ravache, Y.; Aymes-Chodur, C.; Clochard, M.-C.; Coqueret,
798 X.; Cortella, L.; Pellizzi, E.; Rouif, S.; Esnouf, S. In *Ionizing Radiation Effects in*
799 *Polymers*, 2014.
800 43. 55El-Sweify, F. H.; Abdelmonem, I. M.; El-Masry, A. M.; Siyam, T. E.; Abo-
801 Zahra, S. F., Adsorption Behavior of Co(II) and Eu(III) on Polyacrylamide/Multiwalled
802 Carbon Nanotube Composites. *Radiochemistry* 2019, *61* (3), 323-
803 330.10.1134/S106636221903007X
804 44. Abdelmonem, I. M.; Metwally, E.; Siyam, T. E.; El-Nour, F. A.; Mousa, A. R.
805 M., Natural Polymer–Carbon Nanotube Composites Prepared by Gamma Radiation for
806 the Removal of Some Radionuclides. *PhD thesis, Ain Shams* 2019,
807 45. Cheremisinoff, P., Handbook of engineering polymeric materials. CRC Press.
808 1997,
809 46. Tsubokawa, N., Preparation and Properties of Polymer-grafted Carbon Nanotubes
810 and Nanofibers. *Polymer Journal* 2005, *37* (9), 637-
811 655.https://doi.org/10.1295/polymj.37.637
812 47. Wang, J. P.; Chen, Y. Z.; Ge, X. W.; Yu, H. Q., Gamma radiation-induced
813 grafting of a cationic monomer onto chitosan as a flocculant. *Chemosphere* 2007, *66* (9),
814 1752-7.https://doi.org/10.1016/j.chemosphere.2006.06.072
815 48. Hong, T. T.; Hai, L.; Man, N. T.; Tam, T. T.; Ha, P. T. L.; Sam, P. T.; Hang,
816 N. D.; Tu, L. H.; Toan, L. V.; Le Huu, T., The Annual Report, Preparation of poly
817 (acrylic acid)-chitosan hydrogels by gamma irradiation for metal ions sorption.
818 *VINATOM-AR-12-38* 2013, 286-294

49. Hemalatha, P.; Veeraiah, M. K.; Kumar, S. P.; Madegowda, N. M.; Manju, M., Reactivity ratios of N-vinylpyrrolidone-acrylic acid copolymer. *American Journal of Polymer Science* 2014, *4* (1), 16-23.https://doi.org/10.5923/j.ajps.20140401.03
50. Kim, M. K.; Sundaram, K. S.; Iyengar, G. A.; Lee, K. P., A novel chitosan functional gel included with multiwall carbon nanotube and substituted polyaniline as adsorbent for efficient removal of chromium ion. *Chem. Eng. J.* 2015, *267*, 51-64.https://doi.org/10.1016/j.cej.2014.12.091
51. Fathi, Z.; Khavari-Nejad, R.; Mahmoodzadeh, H.; Satari, T., Investigating of a wide range of concentrations of multi-walled carbon nanotubes on germination and growth of castor seeds (Ricinus communis L.). *Journal of Plant Protection Research* 2017, *57*.10.1515/jppr-2017-0032
52. Rajesh, R.; Ravichandran, D., Development of a new carbon nanotube– alginate–hydroxyapatite tricomponent composite scaffold for application in bone tissue engineering. *International Journal of Nanomedicine* 2015, *10*, 7-15.10.2147/IJN.S79971
53. Swain, S. K.; Prusty, K., Biomedical applications of acrylic-based nanohydrogels. *Journal of Materials Science* 2018, *53* (4), 2303-2325.10.1007/s10853-017-1726-x
54. Gokila, S.; Gomathi, T.; Sudha, P. N.; Anil, S., Removal of the heavy metal ion chromiuim(VI) using Chitosan and Alginate nanocomposites. *International Journal of Biological Macromolecules* 2017, *104*, 1459-1468.https://doi.org/10.1016/j.ijbiomac.2017.05.117
55. Liu, Y.; Gao, L.; Sun, J., Noncovalent Functionalization of Carbon Nanotubes with Sodium Lignosulfonate and Subsequent Quantum Dot Decoration. *The Journal of Physical Chemistry C* 2007, *111* (3), 1223-1229.10.1021/jp066018z
56. Murthy, K.; Gowrishankar, B., Process optimisation of methylene blue sequestration onto physical and chemical treated coffee husk based adsorbent. *SN Applied Sciences* 2020, *2*.10.1007/s42452-020-2603-9
57. Robati, D.; Mirza, B.; Rajabi, M.; Moradi, O.; Tyagi, I.; Agarwal, S.; Gupta, V., Removal of hazardous dyes-BR 12 and methyl orange using graphene oxide as an adsorbent from aqueous phase. *Chemical Engineering Journal* 2016, *284*, 687-697
58. Al-Degs, Y. S.; El-Barghouthi, M. I.; El-Sheikh, A. H.; Walker, G. M., Effect of solution pH, ionic strength, and temperature on adsorption behavior of reactive dyes on activated carbon. *Dyes and Pigments* 2008, *77* (1), 16-23.https://doi.org/10.1016/j.dyepig.2007.03.001
59. Dehghani, M. H.; Ghadermazi, M.; Bhatnagar, A.; Sadighara, P.; Jahed-Khaniki, G.; Heibati, B.; McKay, G., Adsorptive removal of endocrine disrupting bisphenol A from aqueous solution using chitosan. *Journal of Environmental Chemical Engineering* 2016, *4* (3), 2647-2655
60. Salleh, M. A. M.; Mahmoud, D. K.; Karim, W. A. W. A.; Idris, A., Cationic and anionic dye adsorption by agricultural solid wastes: A comprehensive review. *Desalination* 2011, *280* (1), 1-13.https://doi.org/10.1016/j.desal.2011.07.019
61. Eren, Z.; Acar, F. N., Adsorption of Reactive Black 5 from an aqueous solution: equilibrium and kinetic studies. *Desalination* 2006, *194* (1), 1-10.https://doi.org/10.1016/j.desal.2005.10.022

62. El-Latif, M. A.; Ibrahim, A. M.; El-Kady, M., Adsorption equilibrium, kinetics and thermodynamics of methylene blue from aqueous solutions using biopolymer oak sawdust composite. *Journal of American science* 2010, *6* (6), 267-283
63. Vijayakumar, G.; Tamilarasan, R.; Dharmendirakumar, M., Adsorption, Kinetic, Equilibrium and Thermodynamic studies on the removal of basic dye Rhodamine-B from aqueous solution by the use of natural adsorbent perlite. *Journal of Materials and Environmental Science* 2012, *3*.ISSN: 2028-2508
64. Freundlich, H. M. F., Über die adsorption in losungen (Adsorption in Solution). *Phys. Chem.* 1906, *57*, 1100–1107.https://doi.org/10.1515/zpch-1907-5723
65. Langmuir, I., The constitution and fundamental properties of solids and liquids. Part II.—Liquids. *J. Frankl. Inst.* 1917, *184* (5), 174.https://doi.org/10.1016/s0016-0032(17)90088-2
66. Temkin, M.; Pyzhev, V., Kinetics of Ammonia Synthesis on Promoted Iron Catalysts. *Acta Physicochimica U.R.S.S* 1940, *12*, 327-356.NII Article ID (NAID): 20000744365
67. Mohammadi, A.; Veisi, P., High adsorption performance of β-cyclodextrin-functionalized multi-walled carbon nanotubes for the removal of organic dyes from water and industrial wastewater. *Journal of Environmental Chemical Engineering* 2018, *6* (4), 4634-4643.https://doi.org/10.1016/j.jece.2018.07.002
68. Zare, K.; Sadegh, H.; Shahryari-ghoshekandi, R.; Maazinejad, B.; Ali, V.; Tyagi, I.; Agarwal, S.; Gupta, V. K., Enhanced removal of toxic Congo red dye using multi walled carbon nanotubes: Kinetic, equilibrium studies and its comparison with other adsorbents. *Journal of Molecular Liquids* 2015, *212*, 266-271.https://doi.org/10.1016/j.molliq.2015.09.027
69. Abualnaja, K. M.; Alprol, A. E.; Abu-Saied, M. A.; Ashour, M.; Mansour, A. T., Removing of Anionic Dye from Aqueous Solutions by Adsorption Using of Multiwalled Carbon Nanotubes and Poly (Acrylonitrile-styrene) Impregnated with Activated Carbon. *Sustainability* 2021, *13* (13).https://doi.org/10.3390/su13137077
70. Yao, Y.; Bing, H.; Feifei, X.; Xiaofeng, C., Equilibrium and Kinetic Studies of Methyl Orange Adsorption on Multiwalled Carbon Nanotubes. *Chem. Eng. J.* 2011, *170*, 82-89.https://doi.org/10.1016/j.cej.2011.03.031